Pump-power dependence due to parametric amplification of the Rayleigh-type optical-mixing signal

J. L. Paz, H. J. Franco, and I. Reif
Escuela de Química, Universidad Central de Venezuela, Caracas 47102, Venezuela

A. Marcano O. and F. García-Golding*
Centro de Física, Instituto Venezolano de Investigaciones Científicas (IVIC), Apartado 21827, Caracas 1020A, Venezuela

(Received 27 July 1987)

A strong pump-power dependence of the Rayleigh-type optical-mixing signal for a water solution of malachite green is reported. Experimental evidence of an exponential pump-power dependence is given. The essential characteristics of the pump-power dependence and the frequency spectrum of the nonlinear signal are qualitatively reproduced by a theoretical model where coupling between pump, probe, and signal fields and propagation effects are considered.

INTRODUCTION

Four-wave-mixing experiments have been used to extract spectroscopic information such as the longitudinal relaxation time (T_1) and the phase-memory or transversal relaxation time (T_2).[1-4] In these experiments nearly copropagating waves of different or equal frequencies interact with the medium generating a nonlinear signal. Different and complicated processes take place during the nonlinear interaction between the field and the matter. In general, there are two types of nonlinear effects. The first ones refer to the local phenomena such as saturation and population oscillations (local effects). The second ones are the result of the coupling interaction between the different components of the field (propagation effects).

Strong-coupling processes, such as parametric amplification of the signal, are expected for high light intensities. The process of four-wave parametric amplification has been treated theoretically by several authors.[5-9] Four-wave parametric amplification when the coupling is due to the molecular-orientation Kerr effect has been reported.[10] Parametric amplification in gaseous media has been also observed.[11]

The study of four-wave parametric amplification in dye solutions is of great interest because of the possible applications in the design of a tunable parametric oscillator.

In this paper we report experimental evidence of a strong power dependence of the nonlinear signal generated in solutions of the organic dye malachite green. For the observation of the nonlinear interaction we use a particular scheme of four-wave mixing: Rayleigh-type optical mixing (RTOM).[2,3,12]

A study of the pump-power dependence of the RTOM signal for different values of the frequency difference $\Delta=\omega_1-\omega_2$, where ω_1 and ω_2 are, respectively, the pump and probe frequencies, was made.

Our data show an exponential pump-power dependence for $\Delta=4$ cm^{-1}. The strength of this exponential dependence changes with the sign of Δ. As a consequence, the width of the RTOM spectrum decreases when the pump power increases.

Strong coupling among the fields and propagation effects have to be considered when explaining the observed exponential pump-power dependence. It is known that parametric amplification can lead to exponential spatial dependence.[5] We show that it can also lead to exponential pump-power dependence.

A theoretical model, which has been used to predict four-wave-mixing parametric amplification in a two-level atomic vapor,[9] gives results which agree qualitatively with our observed experimental behavior.

EXPERIMENTAL RESULTS

The experimental setup consists of two dye lasers (Molectron DL200) pumped by a N_2 laser (Molectron UV1000). The dye lasers have wavelengths tuned near 610 nm and work with a repetition rate of 15 pulses per second. The pulses are 6 ns in length and have a spectral linewidth of 0.5 cm^{-1}. The probe beam (ω_2) was about 10 times weaker than the pump beam. The two beams overlap inside a glass sample cell (0.05-mm internal width) focused by a 20-cm lens. The intensity of the pump beam is accurately set by a continuous, variable attenuator. The pulse energy is measured by a LP141 Molectron detector. The polarization is the same for the signal, the pump, and the probe. We use samples of 5×10^{-4} M solution of malachite green in water. The use of water as the solvent avoids the thermal grating effect.

Two types of experiments are carried out with the setup described above. First we measure the pump-power dependence of the RTOM signal for several values of the frequency difference $\Delta=\omega_1-\omega_2$. Then we measured the RTOM spectra for different values of the pump power. The experimental results are shown in Figs. 1 and 2.

In Fig. 1 the pump-power dependences of the RTOM signal are plotted for different values of Δ. Figure 1(a)

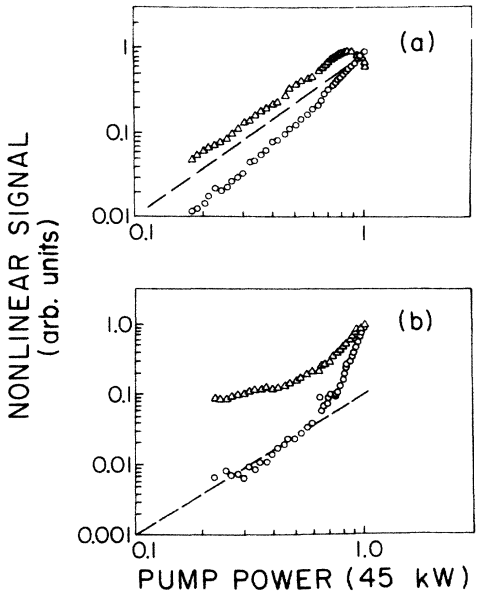

FIG. 1. Pump-power dependence of the RTOM signal for a 0.5-mM water solution of malachite green for different values of the frequency difference $\Delta=\omega_1-\omega_2$. (a) corresponds to $\Delta=+2$ cm^{-1} (circles) and $\Delta=-2$ cm^{-1} (triangles). (b) corresponds to $\Delta=+4$ cm^{-1} (circles) and $\Delta=-4$ cm^{-1} (triangles). The dashed line shows a quadratic dependence.

corresponds to $\Delta=\pm2$ cm^{-1}, and Fig. 1(b) to $\Delta=\pm4$ cm^{-1}.

The dashed line corresponds to a second-order power dependence. The pump-power dependence for positive values of Δ are higher than for negative values.

Of particular interest is the pump-power dependence for $\Delta=4$ cm^{-1} [Fig. 1(b)]. At low power, the dependence is quadratic, but when the pump power increases the dependence becomes higher than quadratic. A detailed analysis of this result shows an exponential growth of the RTOM signal with the pump power.

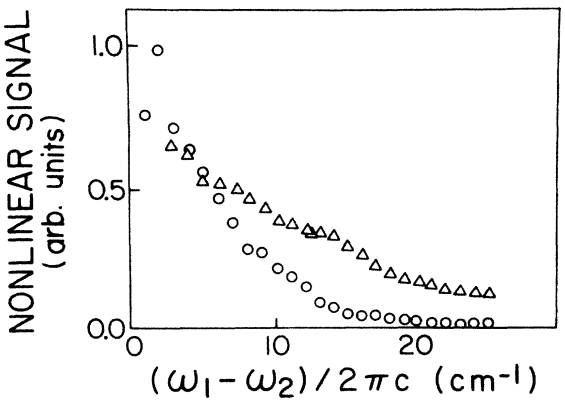

FIG. 2. RTOM spectrum of a water solution of malachite green for two values of pump power: 10 kW (triangles) and 45 kW (circles). Note the narrowing of the spectrum when the pump power increases.

A similar effect is observed for the case $\Delta=2$ cm^{-1}. However, the signal growth is not so strong in this case.

For $\Delta=-2$ cm^{-1} at low power we observe again a quadratic power dependence, but when the pump power increases the power dependence shows a saturation behavior. An interesting result is obtained for $\Delta=-4$ cm^{-1}. Here we have again an exponential growth for the RTOM signal, but the power behavior at low power is less than quadratic.

There are two types of effects in the pump-power dependence shown in Fig. 1. At low power the dependence is quadratic corresponding to a third-order RTOM signal quadratic in pump and linear in probe. At high power the power dependence is higher or lower than quadratic depending on the value of the frequency difference Δ.

The general behavior of the pump-power dependence will be better understood once the results obtained from our theoretical model are shown. As we will see below, this behavior shows a competition between saturation and parametric-amplification effects on the RTOM signal.

Figure 2 shows two RTOM spectra for pump powers $P_1=10$ kW and $P_2=45$ kW. Normally, when saturation prevails over other effects the spectrum width increases with pump power.[13,14] In our case we see the opposite effect. The linewidth narrowing of the spectrum is a consequence of the signal parametric amplification.

THEORETICAL CONSIDERATIONS

The molecules of the dye are considered as an ensemble of two-level systems with an energy difference $\hbar\omega_0$. Two laser beams of frequencies ω_1 and ω_2 nearly resonant with the transition frequency ω_0 are incident on the sample.

The density-matrix equations which describe the behavior of the system are

$$\frac{d\rho_D}{dt}=-\frac{2i}{\hbar}(H_{ab}\rho_{ba}-\rho_{ab}H_{ba})-\frac{1}{T_1}(\rho_D-\rho_D^{(0)}) , \tag{1}$$

$$\frac{d\rho_{ba}}{dt}=\frac{d\rho_{ab}^*}{dt}=-\frac{i}{\hbar}H_{ba}\rho_D-\left[\frac{1}{T_2}+i\omega_0\right]\rho_{ba} , \tag{2}$$

$$H_{ba}=-\boldsymbol{\mu}_{ba}\cdot[\,\mathbf{E}_1\exp(-i\omega_1 t)+\mathbf{E}_2\exp(-i\omega_2 t)+\mathbf{E}_3\exp(-i\omega_3 t)+\text{c.c.}\,] , \tag{3}$$

where $\mathbf{E}_m=A_m\hat{\mathbf{e}}_m\exp(i\mathbf{k}_m\cdot\mathbf{r})$, $m=1,2,3$, $\rho_D=\rho_{aa}-\rho_{bb}$, $\rho_D^{(0)}$ denotes the equilibrium value, H_{ba} is the matrix element of the interaction between matter and radiation, $\boldsymbol{\mu}_{ba}$ is the transition moment, A_1 and A_2 are the amplitudes of the electrical fields of the pump and probe waves, A_3 is the amplitude of the electrical field generated at frequency $\omega_3=2\omega_1-\omega_2$, $\hat{\mathbf{e}}_m$ are the unit vectors in the directions of the field polarization, and T_1 and T_2 are the population and phase-memory relaxation times, respectively.

The following relations were obtained for the Fourier components $\rho_{ba}(\omega_3)$, $\rho_{ab}(-\omega_2)$, $\rho_{ba}(\omega_1)$, and $\rho_D(\omega_1-\omega_2)$ in the steady-state and rotating-wave approximations, at all orders in the pump wave but at first order in the probe and signal fields. Contributions from high-frequency terms were not considered.

$$D_2^*\rho_{ab}(-\omega_2)=-i\Omega_1^*\rho_D(\omega_1-\omega_2)+i\Omega_2^*\rho_D^{dc}\ , \tag{4}$$

$$D_1\rho_{ba}(\omega_1)=i\Omega_1\rho_D^{dc}\ , \tag{5}$$

$$D_3\rho_{ba}(\omega_3)=i\Omega_1\rho_D(\omega_1-\omega_2)+i\Omega_3\rho_D^{dc}\ , \tag{6}$$

$$h_1(\Delta)\rho_D(\omega_1-\omega_2)=-2i\Omega_1\rho_{ab}(-\omega_2)+2i\Omega_1^*\rho_{ba}(\omega_3)+2i\Omega_2^*\rho_{ba}(\omega_1)-2i\Omega_3\rho_{ab}(-\omega_1)\ , \tag{7}$$

where $\Omega_i=(\boldsymbol{\mu}_{ba}\cdot\mathbf{E}_i)/2\hbar$ is the Rabi frequency; $D_j=1/T_2+i(\omega_0-\omega_j)$ with $j=1,2,3$; $h_1(\Delta)=1/T_1+i(\omega_2-\omega_1)$; $\Delta=\omega_2-\omega_1$.

For the zero-frequency component of ρ_D we get

$$\rho_D^{dc}=\rho_D^{(0)}\left[\frac{|D_1|^2T_2^2}{|D_1|^2T_2^2+4S_1}\right]\ , \tag{8}$$

where $S_1=|\Omega_1|^2T_1T_2$ is the saturation parameter.

Solving for $\rho_{ba}(\omega_3)$, $\rho_{ab}(-\omega_2)$, and $\rho_{ba}(\omega_1)$ we have

$$\rho_{ba}(\omega_3,\omega_0)=B_3(\omega_0)\Omega_3+\nu_3(\omega_0)\Omega_2^*\ , \tag{9}$$

$$\rho_{ab}(-\omega_2,\omega_0)=B_2^*(\omega_0)\Omega_2^*+\nu_2^*(\omega_0)\Omega_3\ , \tag{10}$$

$$\rho_{ba}(\omega_1,\omega_0)=B_1(\omega_0)\Omega_1\ , \tag{11}$$

where

$$B_3(\omega_0)=i\frac{\rho_D^{dc}}{2D_3}\left[\frac{h_1(\Delta)+2|\Omega_1|^2\left(\frac{1}{D_2^*}-\frac{1}{D_1^*}\right)}{h_1(\Delta)+2|\Omega_1|^2\left(\frac{1}{D_2^*}+\frac{1}{D_3}\right)}\right]\ ,$$

$$\nu_3(\omega_0)=\frac{-i\Omega_2^2\rho_D^{dc}\left(\frac{1}{D_1}+\frac{1}{D_2^*}\right)}{D_3\left[h_1(\Delta)+2|\Omega_1|^2\left(\frac{1}{D_1^*}+\frac{1}{D_3}\right)\right]}\ ,$$

$$B_2^*(\omega_0)=\frac{-i\rho_D^{dc}}{2D_2^*}\left[\frac{h_1(\Delta)-2|\Omega_1|^2\left(\frac{1}{D_1}-\frac{1}{D_3}\right)}{h_1(\Delta)+2|\Omega_1|^2\left(\frac{1}{D_2^*}+\frac{1}{D_3}\right)}\right]\ ,$$

$$\nu_2^*(\omega_0)=\frac{i\Omega_1^2\rho_D^{dc}\left(\frac{1}{D_1^*}+\frac{1}{D_3}\right)}{D_2^*\left[h_1(\Delta)+2|\Omega_1|^2\left(\frac{1}{D_2^*}+\frac{1}{D_3}\right)\right]}\ ,$$

$$B_1(\omega_0)=i\frac{\rho_D^{dc}}{2D_1}\ .$$

A physical interpretation can be given to each one of the terms in Eqs. (9) and (10).

For instance, the term $\nu_3\Omega_2^*$ in Eq. (9) corresponds to scattering of the pump beam with the wave vector $\mathbf{K}_1$ with the grating with the wave vector $\mathbf{K}_1-\mathbf{K}_2$ formed by the pump and the probe.

The signal measured in the laboratory is proportional to the square modulus of the complex polarization:

$$\mathbf{P}(\omega_j)=N\int_{-\infty}^{\infty}\langle\rho_{ba}(\omega_j)\boldsymbol{\mu}_{ab}\rangle g(\omega_0)d\omega_0\ , \tag{12}$$

where N is the density of absorbent species, $\langle\ \rangle$ denotes the orientational average, and $g(\omega_0)$ is the inhomogeneous distribution of resonant frequencies ω_0.

The following equations give the complex polarization components at ω_3 and ω_2 in the scalar approximation:

$$P_3(\omega_3)=[\chi^{(1)}(\omega_3)E_3+\chi^{(3)}(\omega_3)E_1^2E_2^*]\exp(-i\omega_3t)\ , \tag{13}$$

$$P_2(\omega_2)=[\chi^{(1)}(\omega_2)E_2+\chi^{(3)}(\omega_2)E_1^2E_3^*]\exp(-i\omega_2t)\ , \tag{14}$$

where $\chi^{(j)}(\omega_i)$ (with $j=1,3$ and $i=2,3$) are the intensity-dependent susceptibilities given by

$$\chi^{(1)}(\omega_i)=\frac{\mu_{ba}^2N}{\hbar}B_i^{inh}\ ,$$

$$\chi^{(3)}(\omega_i)=\frac{N\mu_{ba}^2\nu_i^{inh}}{A_1^2\hbar}\ ,$$

where the index (inh) represents the integration over the inhomogeneous distribution. Nonresonant contributions to the nonlinear susceptibilities have not been considered in the model.

These polarizations generate oscillating fields at the same frequency whose propagations are described by the wave equation. In the slow-envelope approximation and considering the pump wave amplitude as a constant (independent of the propagation direction z) we get

$$\frac{dA_3}{dt}=-\alpha_3A_3+\xi_3A_2^*\exp(i\Delta k_zz)\ , \tag{15}$$

$$\frac{dA_2^*}{dt}=-\alpha_2A_2^*+\xi_2^*A_3\exp(-i\Delta k_zz)\ , \tag{16}$$

where

$$\alpha_k=\frac{2\pi\omega_k}{\eta_kC}\,\mathrm{Im}\chi^{(1)}(\omega_k)\ ,$$

$$\xi_k=\frac{2\pi i\omega_k}{\eta_kC}\chi^{(3)}(\omega_k)A_1^2\ ,$$

$$\eta_k^2=1+4\pi\,\mathrm{Re}\chi^{(1)}(\omega_k)\ .$$

Δk is the z component of the propagation-vector mismatch

$$\Delta\mathbf{k}=2\mathbf{K}_1-\mathbf{K}_2-\mathbf{k}_3\ ,$$

which can be written as

$$\Delta k=\frac{\omega}{c}[2\eta_1-(\eta_2+\eta_3)\cos\theta]\ ,$$

where θ is the angle between $\mathbf{k}_1$ and $\mathbf{k}_2$. The coefficient α_k is the absorption coefficient at frequency ω_k in the material medium in the presence of the pump beam. The coefficients ξ_2 and ξ_3 represent the coupling parameters between the probe field and the signal. From the definition of $\chi^{(1)}(\omega_k)$ and $\chi^{(3)}(\omega_k)$ we see that both pa-

rameters are proportional to the linear absorption coefficient α_0,

$$\alpha_0=\frac{2\pi}{\lambda}\frac{\mu_{ba}^2 N}{\hbar}T_2 \ . \tag{17}$$

Solving the coupled equations (15) and (16) we get

$$A_3(z)=\frac{\xi_3 A_2^{(0)*}}{2k_{\text{eff}}}[\exp(g_+z)-\exp(g_-z)]\exp(i\Delta k/2) \ , \tag{18}$$

$$A_2^*(z)=\frac{A_2^{(0)*}}{2k_{\text{eff}}}\left[\left[\frac{i\Delta k}{2}-\alpha_2\right][\exp(g_+z)-\exp(g_-z)] -g_-\exp(g_+z)+g_+\exp(g_-z)\right] \times\exp(-i\Delta kz/2) \ , \tag{19}$$

with

$$k_{\text{eff}}=\tfrac{1}{2}[(\alpha_2-\alpha_3+i\Delta k)^2+4\xi_3\xi_2^*]^{1/2}$$

and the gain coefficient

$$g_\pm=\pm k_{\text{eff}}-\tfrac{1}{2}(\alpha_2+\alpha_3) \ .$$

The appropriate boundary conditions $A_3(0)=0$ and $A_2(0)=A_2^{(0)}$ were used in deriving these results. The RTOM signal intensity is given by

$$I=\frac{4\pi}{c}\,|\,A_3(z)\,|^2 \ . \tag{20}$$

The essential characteristics of RTOM parametric amplification and the role of the saturation are qualitatively illustrated by this model despite the fact that a constant pump-power approximation has been made.

Figure 3 exhibits the pump-power dependence of the nonlinear signal for different values of the parameter $B=\alpha_0 l$, where α_0 is the linear absorption coefficient given by Eq. (17) and l is the cell length. The calculation was done at the center of the RTOM spectrum, for an inhomogeneous Gaussian distribution of linewidth 800 cm^{-1} half width at half maximum (HWHM), with $T_1=2.5\times10^{-12}$ sec and $T_2=0.5\times10^{-12}$ sec. These parameters are in good agreement with picosecond recovery dynamics[15] and saturation measurements[13] in solutions of malachite green.

Initially we observe a quadratic power dependence for all cases corresponding to a third-order RTOM signal quadratic in pump and linear in probe. For small values of B, saturation effects are the important ones. As B increases, parametric-amplification effects become more important and the pump-power dependence becomes higher than quadratic. Eventually it becomes exponential. For values of B (high-absorption case) larger than the ones shown in Fig. 3, we expect the effect of the pump absorption to become important enough to avoid the parametric amplification of the signal, and again the pump saturation could induce a power dependence lower than quadratic. Experimental evidence of this behavior for high-absorption values has been reported in the literature.[12] We cannot observe this behavior theoretically since our model does not allow pump absorption along the cell length.

Figure 4 shows the narrowing of the RTOM spectrum under a pump-power regime higher than quadratic. Again, this effect is opposite to the one expected when only saturation effects are present. The calculation was done with the same parameters of Fig. 3.

As we have seen, the theory agrees qualitatively with our experimental results. However, the theoretical results do not have the frequency-difference-dependent asymmetry which characterizes the observed values shown in Fig. 1.

A model which includes pump depletion by absorption and possible asymmetry-generating factors is now under

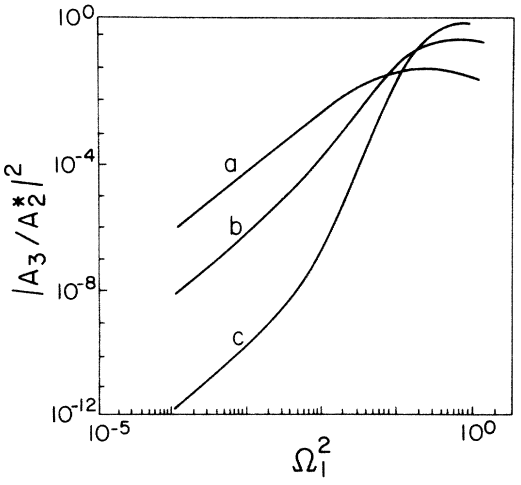

FIG. 3. Theoretical pump-power dependence of the RTOM-signal initial probe-beam-intensity ratio for different values of the parameter $B=\alpha_0 l$: $B=1$ (curve a), $B=5$ (curve b) and $B=10$ (curve c).

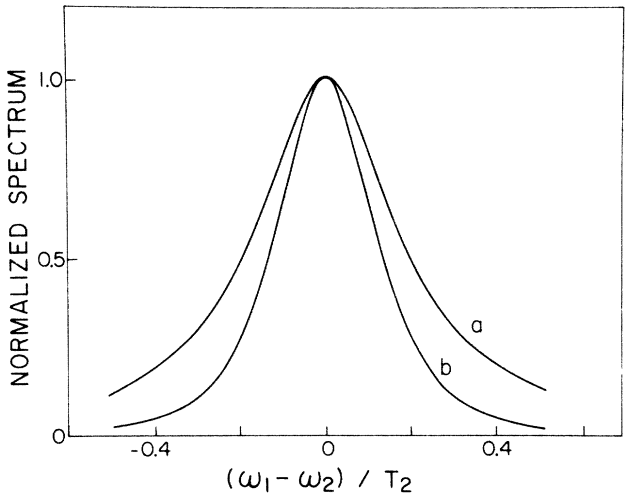

FIG. 4. Theoretical RTOM spectrum for two values of the parameter Ω_1: $\Omega_1=0.05$ (curve a) and $\Omega_1=0.25$ (curve b).

study. These results will be given in a future communication.

CONCLUSIONS

The strong pump-power dependence of the RTOM signal for a water solution of malachite green is reported for the first time. Experimental evidence of an exponential pump-power dependence is given.

The essential characteristics of the pump-power dependence and of the frequency spectrum of the nonlinear signal are qualitatively reproduced by using a two-level inhomogeneously broadened model, to all orders in the pump field and first order in the signal and probe fields. Coupling among the field components and propagation effects are considered but with a constant pump-intensity approximation. This model does not include nonresonant contributions to the material response and does not yield the frequency-difference-dependent asymmetry shown by the experimental results.

Propagation effects are necessary for the observation of an exponential pump-power dependence. Local effects are not enough. Therefore, the optical length should not be too short. On the other hand, a long optical length is not convenient, since then the pump depletion may be too large.

Work is under way to improve our model so that pump absorption and frequency-difference asymmetry are considered.

ACKNOWLEDGMENT

This work was supported in part by Consejo Nacional de Investigaciones Científicas y Tecnológicas, Caracas, Venezuela.

---

*Permanent address: INTEVEP S.A., apartado 76343, Caracas 1070A, Venezuela.

[1]T. Yajima, Opt. Commun. **14**, 378 (1975).

[2]T. Yajima and H. Souma, Phys. Rev. A **17**, 309 (1978).

[3]T. Yajima, H. Souma, and Y. Ishida, Phys. Rev. A **17**, 324 (1978).

[4]H. Souma, T. Yajima, and Y. Taira, J. Phys. Soc. Jpn. **48**, 2040 (1980).

[5]R. Y. Chiao, P. L. Kelley, and E. Garmine, Phys. Rev. Lett. **17**, 1159 (1966).

[6]M. J. Pellin and J. T. Yardley, IEEE J. Quantum Electron. **13**, 904 (1977).

[7]B. R. Mollow, Phys. Rev. A **7**, 1319 (1973).

[8]R. W. Boyd, M. G. Raymer, P. Narum, and D. J. Harter, Phys. Rev. A **24**, 411 (1981).

[9]R. L. Carman, R. Y. Chiao, and P. L. Kelley, Phys. Rev. Lett. **17**, 1281 (1966).

[10]F. Y. Wu, S. Ezekiel, M. Ducloy, and B. R. Mollow, Phys. Rev. Lett. **38**, 1077 (1977).

[11]D. Harter, P. Narum, M. G. Raymer, and R. W. Boyd, Phys. Rev. Lett. **46**, 1192 (1981).

[12]F. García-Golding and A. Marcano O., Phys. Rev. A **32**, 1526 (1985).

[13]A. Marcano O. and F. García-Golding, J. Chem. Phys. **82**, 1242 (1985).

[14]E. P. Ippen, C. V. Shank, and A. Bergman, Chem. Phys. Lett. **38**, 611 (1976).

[15]V. Sudstrom, T. Gillbro, and H. Bergstron, Chem. Phys. **73**, 439 (1982).